World Conference on
Timber Engineering
Oslo 2023

# EVALUATION OF HARDENING MODELS TO SIMULATE JOINTS IN TIMBER SHEAR WALLS

**Rajan Maharjan[1], Johan Vessby[2], Le Kuai[3]**

**ABSTRACT:** The properties of sheathing-to-framing joints considerably affect the load carrying capacity of a light-frame timber shear wall. A fastener with isotropic or kinematic hardening properties is modelled for the sheathing-to-framing joints with a zero-length element, with coupled properties in two perpendicular (orthogonal translational) directions to avoid the overestimation achieved with an uncoupled alternative. A single fastener experiment is performed to determine the elastic and plastic properties. For both fastener level and wall level modelling, monotonic as well as cyclic loading scheme is analysed. A concept of modelling the elasto-plastic coupled behaviour with hardening of the connector model for the fasteners is suggested. A damage response of the fastener is also studied to estimate the failure in load capacity of the connector model and decrease in the wall capacity after the maximum loading.

**KEYWORDS:** Light-frame timber shear wall, Sheathing-to-framing joints, Single fastener test, Connector model

## 1 INTRODUCTION

A timber shear wall is built by timber frame members, studs and rails, and sheathing panels attached together by means of mechanical fasteners. The walls are common in multi-story timber buildings since they act as structural diaphragms and transfer lateral loads like wind and seismic loads to the foundation by in-plane action. Furthermore, they are lightweight and can be pre-fabricated at highly automated indoor facilities at high speed in an efficient manner.

From previous studies e.g. [1, 2], it is observed that the mechanical fasteners used as sheathing-to-framing connections are the most important elements affecting the in-plane stiffness and load carrying capacity of the light-frame timber shear wall. To fully comprehend the response of the wall subjected to the in-plane loading, it is essential to study the behaviour of the fasteners used in such connections, a topic that has been addressed by several researchers during the last decades. These include studies with assumed linear elastic response [3] and plastic response [4] of the fastener as well as simulations based on characteristics from Eurocode expressions [5].

The laterally loaded sheathing-to-framing connections are generally timber-steel-timber connections that undergo elasto-plastic deformation when subjected to the loading. A typical mechanical fastener initially behaves elastic up to the yield force and a plastic displacement develops beyond that force. Further displacement beyond the yield initiation is referred to as 'hardening' if the force is increased and 'softening' if the force decreases.

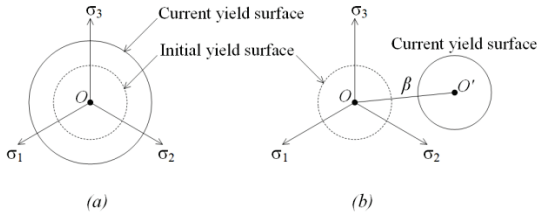


***Figure 1:*** *Initial and current yield surfaces for (a) isotropic and (b) kinematic hardening in the deviatoric plane.*

Hardening can be classified as isotropic hardening or kinematic hardening [6] and they may both be used to simulate the plastic behaviour of the fasteners. The initial yield surface and current yield surfaces for isotropic and kinematic hardening are shown in Figure 1 in the deviatoric plane, perpendicular to the hydrostatic axis.

With an increase in loading, if the subsequent yield surface expands uniformly in all direction in the stress space, the hardening is isotropic. When the yield surface shifts in the stress space, without change in the shape while loading and unloading, the hardening is kinematic. In Figure 1(b), the shift perpendicular to the hydrostatic axis of the current yield field space $\beta$ is termed as back-stress. For a typical fastener of the type studied, plastic deformation proceeds the failure of the joint. The failure in turn may occur pre or post the average peak load of the fastener type. The peak load is the maximum load registered in the fastener during an experimental test.

Several studies were performed previously on various fasteners to study the performance of mechanical fasteners under monotonic or cyclic loading. Models for

[1] Rajan Maharjan, Karlstad University, Sweden, rajan.maharjan@kau.se
[2] Johan Vessby, Karlstad University, Sweden, johan.vessby@kau.se
[3] Le Kuai, Linnaeus University, Sweden, le.kuai@lnu.se


https://doi.org/10.52202/069179-0354

both monotonic and cyclic lateral behaviours of the nail connection was established in the 1990s e.g. [7]. A hysteresis model, based on modification of the Bouc, Wen, Baber and Noori model, was used [8] in non-linear dynamic analysis of a single-degree-of-freedom wood systems. It was modified to a non-linear and history dependent hysteretic behaviour of a nailed joint [2] which was performed using an user defined element in the finite element (FE) based software ABAQUS.

A recent study on modelling the fastener with a coupled zero-length element was applied on seismic analysis of wood-frame structures [9]. The coupled properties of the zero-length element were implemented to avoid an overestimation of the forces when the load is applied in two orthogonal directions simultaneously. Such coupling may be performed in various ways and some of those are scrutinized by [10]. As previously stated, an accurate model of the fastener is crucial for a correct simulation of a whole shear wall. Many of the previous studies on fasteners also include simulations of different types of shear walls and conclude that the fastener model works well for the wall level e.g. [11].

The aim with the current paper is to evaluate any possible effect in the load-displacement response of choosing an isotropic or kinematic hardening model for the fasteners. To do so, they are modelled in a FE-software using a zero-length coupled element under monotonic and cyclic loading in a 2-D space. The study is performed for a single fastener and for a three panelled shear wall unit. The pinching effect in the cyclic loading is not considered in the simulations performed. An analysis of the damage response of the fasteners is also performed both for the single fastener level and the shear wall level.

# 2 MATERIAL AND METHODS

## 2.1 EXPERIMENTAL STUDY

For the experimental study, a timber frame, 45·120 mm in cross-section and of strength class C24 are used. Furthermore, a 12 mm plywood sheathing panel of quality K20/70 and a 3.9·55 mm screw were used for the single fastener test. Monotonic and cyclic tests were performed according to EN 12512 [12] for a single fastener to obtain the load displacement curves and to study a typical loading cycle of the fastener which is loaded parallel to the fibre direction of the timber member.

### 2.1.1 Monotonic test of a single fastener

A screw was fastened to the sheathing panel (plywood 250·100·12 mm) and the frame (C24 and cross section dimensions 120·45 mm) at the distance of 50 mm from the closest edge in the loading direction, see Figure 2 . The timber frame was fixed to the steel frame by using four Ø 8 mm and 250 mm long steel threaded rods and bolts. The sheathing panel was connected with four bolts, Ø = 4 mm, to the 45·3 mm steel plate that was clamped to the hydraulic wedge grip of the MTS machine having a capacity of ± 100 kN and ± 0.1% linear tolerance interval. The relative displacements between the frame and the panel were acquired by means of two linear variable

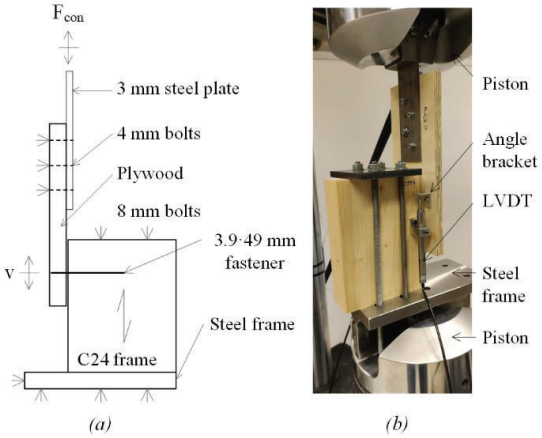


***Figure 2:*** *(a) Setup of the single fastener test and (b) on-going test of the single fastener.*

differential transformers (LVDTs) that were placed at each side of the frame member. The LVDTs were mounted, to the closest possible location of the fastener, on the frame and measured relative to a 15 mm aluminium angle bracket in turn secured to the panel. The monotonic tests were performed under displacement control at a rate of 0.2 mm/sec and from the load-displacement plot of the test the yield displacement $v_y$ was calculated. For the load displacement curve having two clearly linear components, the yield values are determined from the intersection of the two lines according to the procedure suggested in EN 12512 [12].

### 2.1.2 Cyclic test of a single fastener

The cyclic tests were also performed in the same setup with the load protocol illustrated in Figure 3 where $v_y$ is the yield displacement determined from the monotonic test. The first cycle consists of compression load (towards the steel frame) until the LVDT displacement of $0.25 \cdot v_y$, followed by unloading to zero displacement,

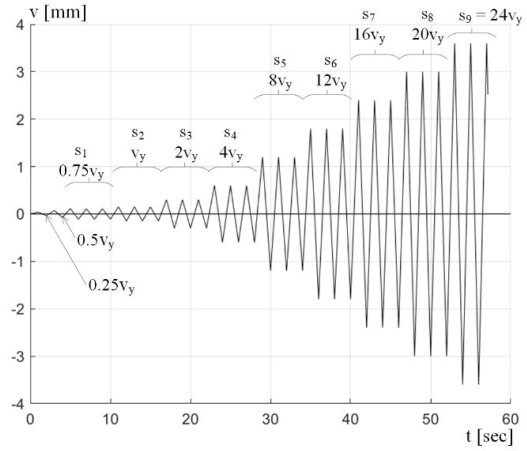


***Figure 3:*** *Loading protocol for the cyclic test where $v_y$ is estimated yield displacement calculated from monotonic test.*

reloading to tensile load (away from the steel frame) up to the LVDT displacement of $0.25 \cdot v_y$ and followed again by unloading to the zero displacement. The second cycle consists of similar loading scheme but this time to the maximum displacement of $0.5 \cdot v_y$. A series ($s_1$) of three cycles are introduced thereafter with the maximum displacement of $0.75 \cdot v_y$ and so forth with increasing factors for the maximum displacement until failure or until a maximum displacement of $v$ = 30 mm is reached. For both monotonic and cyclic tests, the test frame and the sheathing panel were placed inside a climate chamber with controlled temperature of 20°C and relative humidity of 65% prior to the test, to secure a moisture content around 12% in the timber. The screw was driven by an electric screwdriver after the test setup was prepared.

## 2.2 NUMERICAL STUDY

### 2.2.1 FEM model of the single fastener

A two-dimensional connector model of the zero-length element consisting of two orthogonal coupled springs was developed for simulation of the fastener in the commercial FE software ABAQUS. The linear elastic and the non-linear plastic hardening properties of the connector model were assigned based on the results from the cyclic experimental tests. A comparative study on isotropic hardening and kinematic hardening during cyclic loading was performed.

For the isotropic hardening, the yield surface $F^0$ is a function of equivalent plastic relative displacement $\bar{u}^{pl}$ that can be expressed as:

$$F^0 = \bar{F}_0 + Q_{inf}(1 - e^{-b \cdot \bar{u}^{pl}}) \qquad (1)$$

where, $\bar{F}_0$ is the yield force value at zero plastic relative displacement, and $Q_{inf}$ and $b$ are material parameters affecting the shape of the hardening curve.

Similarly, for the kinematic hardening, the change in the backforce over a half cycle of a unidirectional tension or compression experiment is expressed as:

$$F_j = (F_j{}^0 + \beta_j), \qquad \beta = \frac{C}{\gamma}\left(1 - e^{-\gamma \cdot u^{pl}}\right) \qquad (2)$$

where, $F_j{}^0$ is the initial yield force value, $\beta$ is the backforce, $u^{pl}$ is the plastic relative displacement, and $C$ and $\gamma$ are material parameters that are calibrated from the test [13]. The backforce for the connector model is interpreted similar to the back stress in Figure 1(b). The values of $Q_{inf}$ and $b$ for isotropic hardening and $C$ and $\gamma$ for kinematic hardening were determined by plotting the best fit curve to the envelope curve of the cyclic experimental load-displacement relation.

Since the fasteners in the shear walls experience forces in both orthogonal directions, a coupled behaviour of the fastener is desirable. Therefore the plastic properties of the connector model were modelled as coupled for both hardening models studied. The linear elastic stiffness of the connector was defined as $k = 2 \cdot 10^6$ N/m in both orthogonal directions. The yield force for the cyclic test denotes the boundary between linear elastic and non-linear plastic hardening behaviours studied.

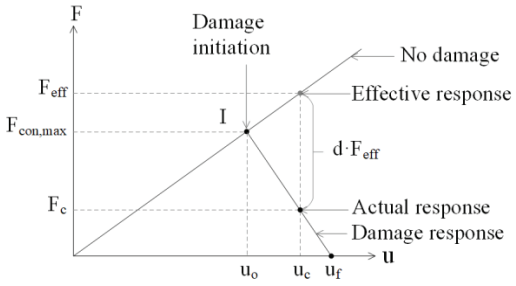


***Figure 4:*** *Damage initiation and damage response.*

When the force in the connector model that is under plastic hardening exceeds its critical value, an irreversible damage is initiated and additional loading leads to further evolution of damage, eventually leading to failure of the fastener. The force response of the connector component $i$ when damage take place is determined as

$$F_i = F_{effi}(1 - d_i), \qquad 0 \le d_i \le 1 \qquad (3)$$

where, $d_i$ is a scalar damage variable and $F_{effi}$ is the effective response in the available connector component under assumption of no damage.

Figure 4 illustrates a simple linear elastic response of a fictive connector with and without damage response. If damage is not defined, the effective response is when the force in the connector is $F_{eff}$ at a displacement $u_c$. When a damage initiation is introduced at point I by using a damage criteria, the corresponding displacement is $u_o$. After the connecter is loaded more so that the displacement increase to $u_c$, the connector force reduces to the current force as determined in Equation (3) depending upon the value of $d$. Further loading of the connector gradually reduces the response, leading subsequently to the ultimate failure displacement $u_f$. At the failure displacement, $d$ = 1, which is its maximum value, and at this point the connector loses the ability to carry any load [13].

A force-based damage initiation criterion was specified by defining the lower or compression limit $F_{con,min}$ and the upper or tension limit $F_{con,max}$ for the damage initiation force values. The limits were determined from the maximum load carrying capacity of the fastener from the cyclic tests. Since coupled connector are used, when the resultant of the forces in the connector between two orthogonal directions is outside the range of the two limit values for the first time, the damage initiation occurs. In addition, a linear evolution law is defined by specifying a relative displacement $u_{dam}$ which is the difference between the relative displacement at ultimate failure and the relative displacement at damage initiation $u_{dam} = u_f - u_o$. It describes the additional linear deformation after the damage initiation for the connector to reach the zero force level. A small value of $u_{dam}$ indicates that the connector has brittle property and on the contrary if $u_{dam}$ is large the failure behaviour in the connector is more ductile.


https://doi.org/10.52202/069179-0354

### 2.2.2 FEM model of simple light-frame shear wall

A shear wall 3.6·3.0 m$^2$ with three wall panels of width 1.2 m was modelled in a 2-D space with C24 timber frames (cross section 45·120 mm) as beam elements and 12 mm plywood panels as shell elements. The sheathing-to-framing joints for 3.9·55 mm mechanical fasteners were modelled by using one of the two aforementioned connector models. The centre-to-centre spacing between the fasteners at the outer edges of the sheathing panels was assigned as $s$ = 100 mm and that for the intermediate stud at the middle of the panel was assigned as $s_{mid}$ = 200 mm, see Figure 5. The connections between the rails and the studs, which generally consist of 2-3 nails of dimensions 3.1·90 mm, were modelled as a hinge joint so that only the effect of sheathing-to-framing fasteners could be assessed for the global behaviour of the wall. The bottom rail of the wall was fixed to the ground and a displacement controlled horizontal load $F_w$ was applied at the left end of the top rail. A monotonic loading up to a prescribed displacement $u_{pres}$ and a cyclic loading with different displacement amplitude were applied to analyse the global behaviour and the local fastener behaviour. Results from the models were used to compare load-displacement curves for the two hardening models, and to illustrate forces from all fasteners acting on the wall panel at a current load stage and force history during the whole load event for some selected fasteners.

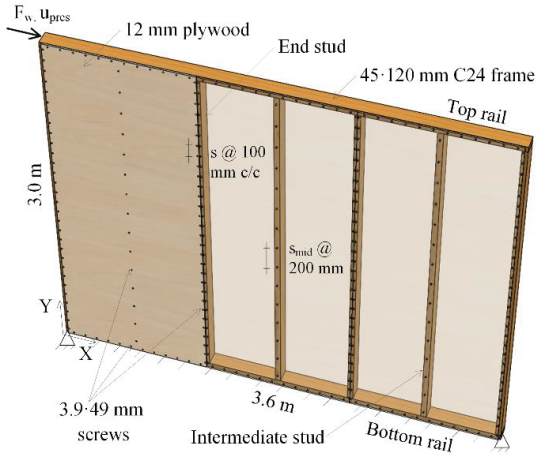


***Figure 5:*** *A simple shear wall model with geometry and spacing of fasteners.*

## 3 RESULT AND DISCUSSION

### 3.1 EXPERIMENTS OF A SINGLE FASTENER

The result of single fastener experimental test is illustrated in terms of load-displacement diagram. The force value is taken from the MTS load cell and the displacement value is taken as an average of the two LVDTs that were placed on each side of the fastener.

Among many monotonic tests performed, a typical test result is illustrated to show the calculation method of the yield displacement. From the single fastener monotonic test, the yield load $F_y$ = 588 N and yield displacement $v_y$ = 0.15 mm were determined from the intersection of the two clearly visible linear components (indicated with dotted lines), see Figure 6. The maximum force experienced by the screw in the load-displacement curve is 2340 N at the displacement 10.4 mm.

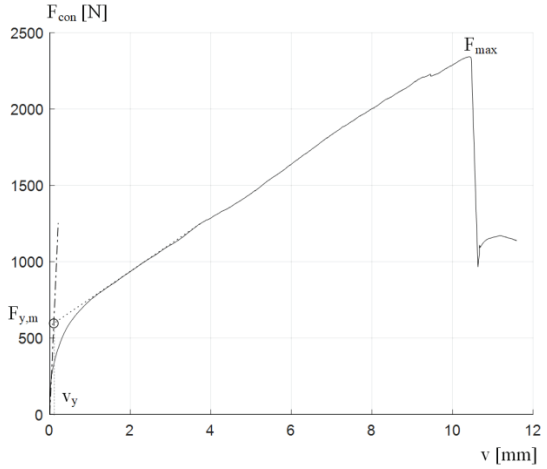


***Figure 6:*** *Load displacement curve from a monotonic test of single fastener showing the yield force $F_y$ from the intersection of two linear components (dotted lines) of the curve.*

Similarly a typical test result from the cyclic loading experiment is shown in Figure 7, which illustrates the load-displacement response for the loading protocol with the yield displacement $v_y$ = 0.15 mm. The experimental data is shifted by + 50 N to the tension zone to adjust the centre of the hysteresis curve about the force axis. The black curve illustrated in the figure is the envelope curve for the test, which is obtained by connecting the force values from the first cycle of each series of the cyclic test, see Figure 3. The envelope response from the cyclic test is observed to yield at $F_y$ = 490 N at a displacement of 0.135 mm, and thus, the elastic modulus is calculated as $k_E$ = 3630000 N/m.

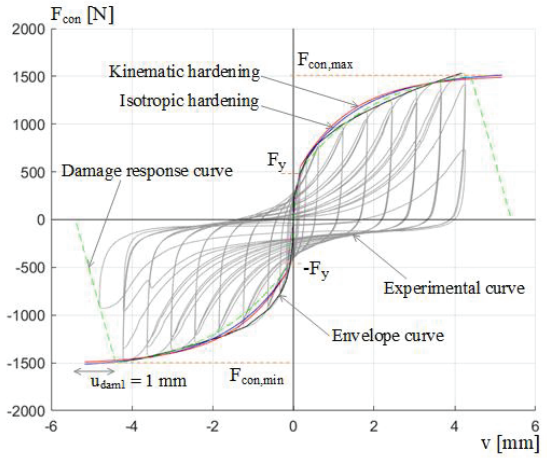


***Figure 7:*** *Load displacement curve for a cyclic loading of the single fastener test with an envelope curve, hardening curves and curves with damage response for $v_y$ = 0.15 mm.*

https://doi.org/10.52202/069179-0354

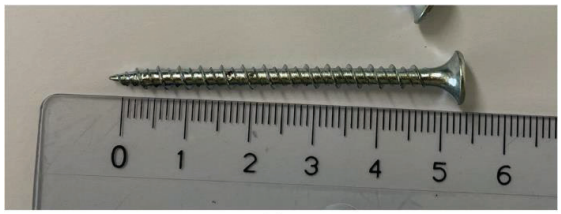


(a)

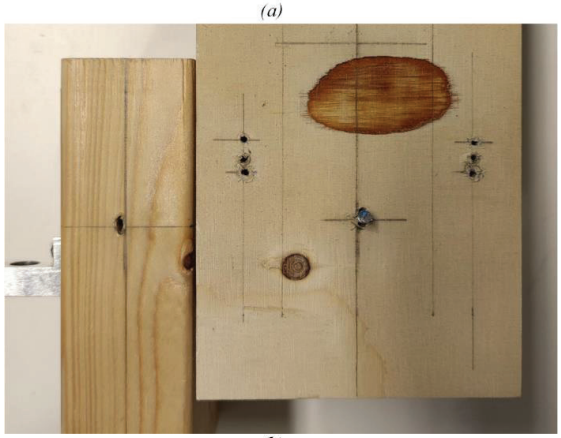

(b)

***Figure 8:*** *The screw (a) before the test and (b) after the ultimate failure in the cyclic test.*

The isotropic hardening parameters are obtained by adjusting the parameters in Equation (1) so that the response fits the envelope curve from the experimental results which occurs for $Q_{inf}$ = 1100 and b = 630.
Similarly the kinematic hardening parameters $C$ = 660000 and $\gamma$ = 590 in Equation (2) are used to fit the experimental results. The lower half-cycle curve for the both hardening properties are obtained by using $F_y$ = - 490 N so that a symmetry in the force-displacement curve is obtained.
From Figure 7, it is observed that during the cyclic test, the screw reached the maximum load carrying capacity $F_{con,max}$ = 1500 N at the cyclic displacement $v$ = 4.2 mm, which is the 10th series of the loading protocol. Therefore, the damage initiation limits, $F_{con,max}$ = 1500 N and $F_{con,min}$ = -1500 N are used for both hardening models. Moreover, two alternate relative displacements $u_{dam1}$ = 1 mm and $u_{dam3}$ = 3 mm are assumed for the connector model which is an estimation of the further deformation of the fastener after the peak load up to the ultimate failure displacement $u_f$ of the fastener. The test screw before and after the ultimate failure from the cyclic test is shown in Figure 8.

### 3.2 MODELLING OF A SINGLE FASTENER

The input parameters for both hardening models are obtained from the cyclic experimental data to model the response of the single fastener. The simulation results for a typical load cycle with the displacement amplitude $v_A$ = 1.2 mm are illustrated in Figure 9 along with the hysteresis curve from the experiment at that amplitude. The amplitude $v_A = 8 \cdot v_y$ is selected from the 5$^{th}$ series of the loading protocol, see Figure 3. The time displacement graph for the model is illustrated in the subfigure where the solid lines represent the load cycle that are extracted for the hysteresis curve. The isotropic hardening model simulated higher force values whereas the kinematic hardening simulated the force values closer to the experimental values at the selected cycle. The shape of the experimental hysteresis curve is similar to the load cycle of the kinematic hardening, provided the simplifications that the pinching effect achieved in the test is not included and only the linear elastic stiffness $k_E$ is considered during the modelling.

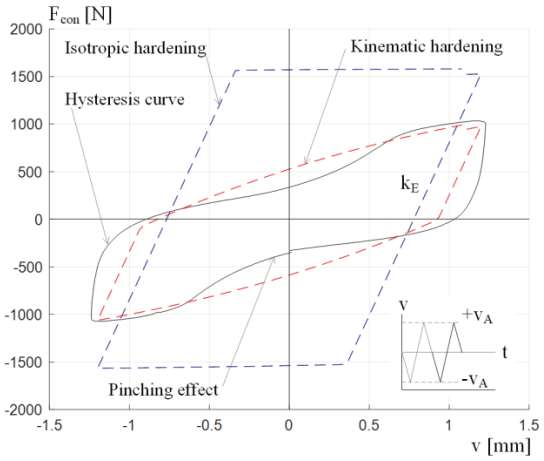


***Figure 9:*** *A typical load cycle at a displacement amplitude of $v_A$ = 1.2 mm from the single fastener cyclic test and models simulating isotropic and kinematic hardening.*

### 3.3 MODELLING OF A SHEAR WALL

The FEM model of the shear wall is used for both the monotonic and the cyclic loading. The monotonic loading for a prescribed displacement, $u_{pres}$, is illustrated in Figure 10 that shows the global behaviour of the wall for both hardening models of the fasteners. The blue curves illustrate the response while isotropic hardening is used in the fasteners and the red curves show the results if kinematic hardening is used for the monotonic loading of the wall. Two curves show the global response of the wall without defining the damage response in the connector model. The load in the wall increases asymptotically for both the hardening models, which is unrealistic from an experiment point of view. The two other loading curves show the global response with the damage initiation limit equal to the maximum load carrying capacity of the fastener from the test, $F_{con,max}$ = 1500 N and the relative displacement $u_{dam1}$ = 1 mm. The damage response on the fasteners resulted in numerical instability in the model at the wall displacement around $u_w$ = 24 mm. The reason for the instability is the significant drop in load carrying capacity of the fasteners (because of the steep gradient) after reaching the peak load, which is also an indication of the brittleness in the fasteners.


https://doi.org/10.52202/069179-0354

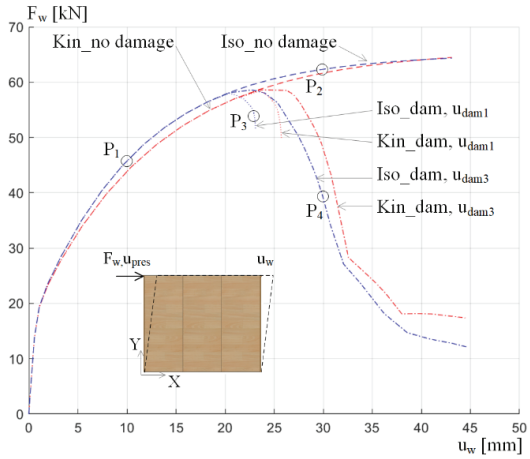


***Figure 10:*** *Load displacement diagram of a shear wall model with damage response $u_{dam1}$, $u_{dam3}$ and without damage response for both hardening models.*

To model the connector with an increased ductility, the damage response of the fasteners is redefined with $u_{dam3}$ = 3 mm, and a third loading is performed. With the increase in the relative displacement, $u_{dam3}$, after the peak load in the connectors, the gradient is not so steep and the response of the wall is added in the load-displacement diagram, see Figure 10.

To comprehend the local phenomenon experienced by the fasteners, vector plots of the connector forces in the wall are plotted at different stages and for different assumptions regarding damage response, as positions marked by circles and denoted as $P_1$-$P_4$ in Figure 10. Since both hardening models showed similar global behaviour in monotonic loading, the force vector plots are presented only for the kinematic hardening model.

Figure 11 (a) and (b) show the vector plots at the position $P_1$ ($u_w$ = 10 mm) and $P_2$ ($u_w$ = 30 mm) respectively for the connector response with no damage defined. The green arrows show scaled vector plot of the forces in the connector at loads lower than the yield load $F_y$ = 490 N and the pink arrows illustrate the vector plot of the forces between $F_y$ and the maximum load carrying capacity of the connector, $F_{con,max}$ = 1500 N. Similarly the red arrows show the vector plot of the connector forces that are greater than $F_{con,max}$. It is observed that the fasteners at the corners of the wall panels reach their peak load first, followed by other fasteners placed close to them. As the displacement in the wall increases, the forces in the connectors also increase and at position $P_2$, most of the connectors have surpassed the defined peak load of the connectors.

Since the experimental results reveal that fasteners fail at $F_{con,max}$ = 1500 N, the wall model is analysed with the damage response on the connector model. Figure 11(c) illustrates the vector plot of the forces on the connectors at the position $P_3$ ($u_w$ = 24 mm), which has the damage response definition by the force limit $F_{con,max}$ and the relative displacement $u_{dam1}$ = 1 mm. The connectors at the

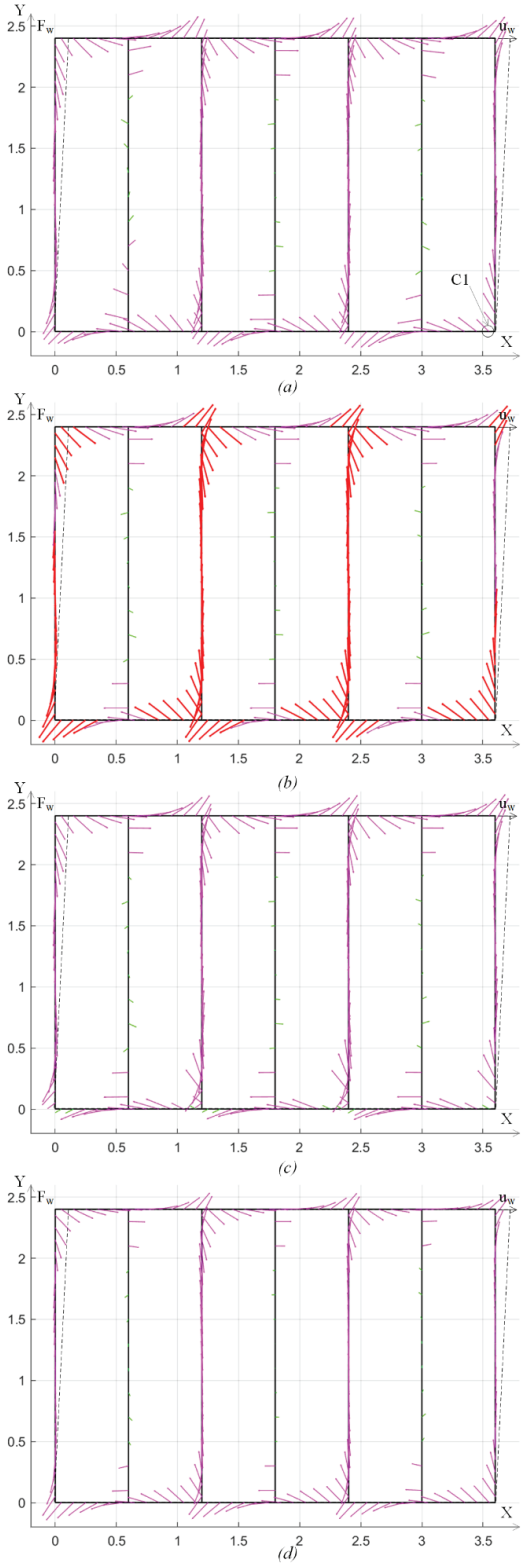


***Figure 11:*** *Force distribution on fasteners of the shear wall model for monotonic displacements at positions (a) $P_1$, (b) $P_2$, (c) $P_3$ and (d) $P_4$ indicated in the Figure 10.*

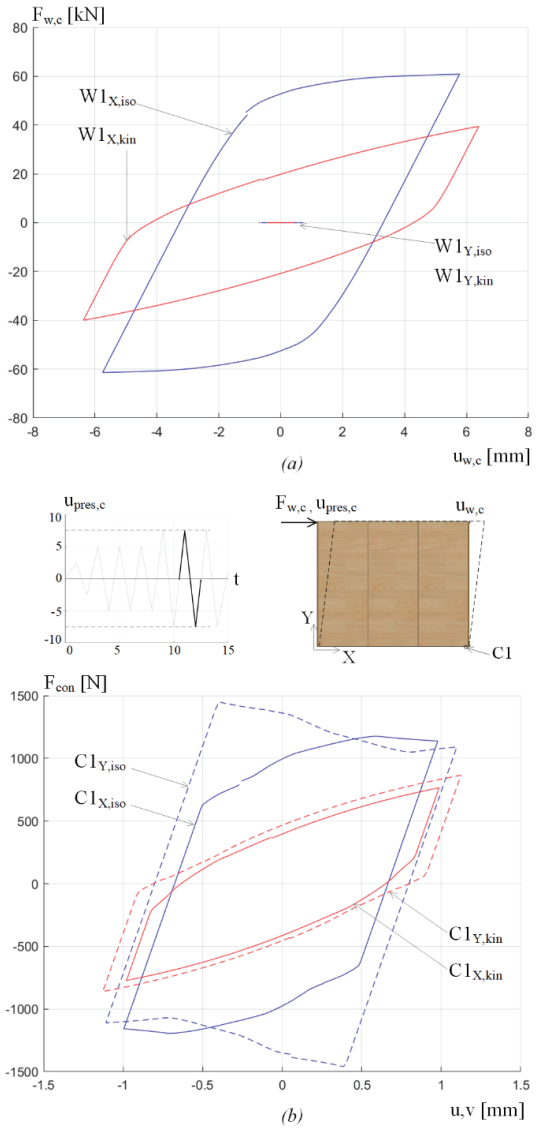


***Figure 12:*** *Load displacement diagram for both hardening models in two orthogonal directions for the displacement amplitude $u_{pres,c}$ = 7.5 mm for (a) shear wall model and (b) for the most loaded fastener denoted C1.*

bottom corners of the three sheathing panels have drastically lower force values, which indicate that they have suffered the damage response the most, thus resulting to the numerical instability.

A comparison of the local connector behaviour is performed for the wall without damage response and with the damage response defined by the force limit $F_{con,max}$ and the relative displacement $u_{dam3}$ = 3 mm. The vector plots for the former is discussed earlier in Figure 11(b) and the latter, at the position *P4* ($u_w$ = 30 mm), is illustrated Figure 11(d). With the damage response $u_{dam3}$, the forces in the connectors don't exceed the maximum load carrying capacity, $F_{con,max}$. Moreover, the most loaded fasteners at the bottom corners of the sheathing panels have surpassed the $F_{con,max}$ and are in the state of decreasing load bearing capacity at that displacement.

The cyclic loading of the wall model is also simulated and the hysteresis curve for the prescribed displacement amplitude $u_{pres,c}$ = ± 7.5 mm is illustrated Figure 12(a) for the isotropic and the kinematic hardening models of the connector in both horizontal and vertical direction. The damage response for the connector models are not defined for the cyclic loading of the wall model. The displacement amplitude is increased from 2.5 mm with scale factors similar to those used for the single connector model, see subfigure. Since the load was applied along the horizontal (*X*) direction, the sum of the reaction force for the wall along the vertical (*Y*) direction is null. The load-displacement response of the wall exhibits similar shape as the connector model for both hardening models. Moreover, the maximum load applied for the wall with isotropic hardening model is higher compared to the maximum load with the kinematic hardening model, which correlates well with the results for the single connector model.

In order to compare the global wall behaviour with the local fastener behaviour, the force-displacement diagram for the most loaded connector *C1*, indicated in Figure 11(a) at the right end of the bottom rail without the damage response, is illustrated in Figure 12(b). Both the connector forces, defined as $F_{con}$ in the *X*- direction and the *Y*- direction, are illustrated in the figure for both hardening models with respect to the connector displacement $u$ and $v$ in the *X* and *Y*- directions respectively. The connector properties are expressed in orthogonal directions, therefore the resultant of the connector force components in orthogonal directions is the total connector force in action. The kinematic hardening of the fastener for the load amplitude used has similar shape in the force-displacement diagram as the wall. The exception is that for the connector with isotropic hardening model, the vertical component $C1_{Y,iso}$ has higher force than at the horizontal component $C1_{X,iso}$.

## 4 CONCLUSIONS

The single fastener experimental tests were used to fit two types of elasto-plastic, zero-length coupled elements to the test results, one using isotropic hardening and the other using kinematic hardening. Both models used for the single fastener simulation and the wall simulation are appealing due to their wide availability, their degree of establishment and their simplicity. The comparison between results from simulation using the two models for plasticity and the experimental results indicate the considerable advantage of using a kinematic hardening model compared to the isotropic one for the current application. A benefit with both models is that different properties may be assigned in the two orthogonal directions so that orthotropy in the timber and in some of the sheathing panels may be included in the simulations. These properties influence results from analysis of shear


https://doi.org/10.52202/069179-0354

walls, in particular when the load directions in the fasteners vary during the loading of the wall.
Furthermore, the shear wall models were simulated with the connector models for monotonic and cyclic loading and it was observed that the shape of the load-displacement curve for the global behaviour of the wall was similar to that of the local behaviour of the connector for the most loaded fastener in the wall.
Moreover, the damage response for the connector model was defined to simulate the decreasing load carrying capacity of the fastener after the peak load and until the failure of the fastener. The suggested method for simulating the damage is efficient and the distinct effect of failure in fasteners on the load carrying capacity in the shear wall is shown.

## 5 FURTHER STUDY

In the current paper, the properties parallel and perpendicular to the fibers are assumed similar. To increase the accuracy of the model, orthotropic properties should be used for the fastener. A series of single fastener experiment for the loading perpendicular to the fibre direction can be performed in order to verify the orthotropic behaviour of the fastener. An experiment on cyclic loading for a simple wall can also be performed to validate the wall model with the zero-length element connector model. Moreover, the effects of large deformation in the connector and the pinching effect of the fasteners can also be included in the further studies.

## ACKNOWLEDGEMENT

The research is financially supported by several wood construction companies in Sweden and by the strategic innovation programme Smart Built Environment and Formas. The authors acknowledge that support with great gratitude.

## REFERENCES

[1] Sartori, T. and R. Tomasi, Experimental investigation on sheathing-to-framing connections in wood shear walls. *Engineering Structures*, 56: p. 2197-2205, 2013.
[2] Xu, J. and J. Dolan, Development of nailed wood joint element in ABAQUS. *Journal of Structural Engineering-ASCE*, 135, 2009.
[3] Källsner, B. and U.A. Girhammar, Analysis of fully anchored light-frame timber shear walls—elastic model. *Materials and Structures*, 42: p. 301-320, 2009.
[4] Källsner, B. and U.A. Girhammar, Plastic models for analysis of fully anchored light-frame timber shear walls. *Engineering Structures*, 31(9): p. 2171-2181, 2009.
[5] Kuai, L., S. Ormarsson, J. Vessby, and R. Maharjan, A numerical and experimental investigation of non-linear deformation behaviours in light-frame timber walls. *Engineering Structures*, 252: p. 113599, 2022.
[6] Ottosen, N.S. and M. Ristinmaa, The Mechanics of Constitutive Modeling. Elsevier Science Ltd: Oxford. p. 247-264, 2005.
[7] Dolan, J.D. and B. Madsen, Monotonic and cyclic nail connection tests. *Canadian Journal of Civil Engineering*, 19(1): p. 97-104, 1992.
[8] Foliente Greg, C., Hysteresis Modeling of Wood Joints and Structural Systems. *Journal of Structural Engineering*, 121(6): p. 1013-1022, 1995.
[9] Di Gangi, G., C. Demartino, G. Quaranta, and G. Monti, Dissipation in sheathing-to-framing connections of light-frame timber shear walls under seismic loads. *Engineering Structures*, 208, 2020.
[10] Vessby, J., E. Serrano, and A. Olsson, Coupled and uncoupled nonlinear elastic finite element models formonotonically loaded sheathing-to-framing joints in timber based shear walls. *Engineering structures*, 32(11): p. 3433-3442, 2010.
[11] Xu, J. and J. Dolan, Development of a wood-frame shear wall model in ABAQUS. *Journal of Structural Engineering-ASCE*, 135, 2009.
[12] EN12512:2001, Timber structures - Test methods - Cyclic testing of joints made with mechanical fasteners: Brussels, Belgium, 2001.
[13] Dassault-Systèmes, Simulia user assistance 2020: Abaqus/cae user's guide: Vèlizy-Villacoublay, France., 2020.